Synthesis, Characterization, and Swelling Behavior Evaluation of Hydrogels Based on *Gum ghatti* and Acrylamide for Selective Absorption of Saline from Different Petroleum Fraction–Saline Emulsions

Balbir Singh Kaith, Rajeev Jindal, Hemant Mittal, Kiran Kumar

Department of Chemistry, Dr. B. R. Ambedkar National Institute of Technology, Jalandhar 144 011 (Punjab), India

Received 8 May 2010; accepted 10 July 2011
DOI 10.1002/app.35238
Published online 25 October 2011 in Wiley Online Library (wileyonlinelibrary.com).

ABSTRACT: In this research article, the synthesis of *Gum ghatti* and acrylamide based superabsorbents under pressure with *N,N′*-methylene bisacrylamide as a crosslinker and an ascorbic acid–potassium persulfate redox pair as an initiator is reported. To study the impact of the different reaction variables on the water absorbance of the candidate polymer, different reaction parameters, including the reaction time, amount of solvent, pH of the medium, initiator ratio, pressure, and monomer and crosslinker concentrations, were optimized. The candidate polymer was characterized with different techniques, including Fourier transform infrared spectroscopy, scanning electron microscopy, thermogravimetric analysis, differential thermal analysis, differential thermogravimetry, and X-ray diffraction. The crosslinked product was found to be thermally more stable than the initial backbone. The swelling capacity of the synthesized polymer was investigated in deionized water as a function of time, temperature, and pH of the swelling medium. Moreover, the effects of the ionic strengths of different cations on the swelling capacity of the candidate polymer were studied with different salt solutions. The tendency of absorbency for these hydrogels in salt solutions was found to be in the following order: $Na^{+} > Ba^{2+} > Fe^{3+} > Sn^{4+}$ for NaCl, $BaCl_2$, $FeCl_3$, and $SnCl_4$ salt solutions. Further, the candidate polymer was used for the selective absorption of saline water from different petroleum fraction–saline emulsions. The results showed that the saline absorption capacities of the hydrogels were 667, 610, 646, and 680% in kerosene–saline, diesel–saline, petrol–saline, and petroleum ether–saline emulsions, respectively. © 2011 Wiley Periodicals, Inc. J Appl Polym Sci 124: 2037–2047, 2012

Key words: crosslinking; hydrogels; polymer synthesis and characterization; swelling; thermogravimetric analysis (TGA)

INTRODUCTION

Superabsorbent hydrogels are the three-dimensional crosslinked polymeric networks that swell in water or biological fluids up to several times their initial volume. They are often sensitive to environmental conditions and can show reversible swelling behavior with changes in the external conditions, such as in the pH, temperature, and electrical stimulus.[1,2] The presence of hydrophilic groups, high polymer chain flexibility, and the availability of a large free volume between polymer chains enhances the swelling capacity of hydrogels.[3] The use of natural polysaccharides in the modification and synthesis of hydrogels has been reported because of their cost effectiveness, biodegradability, and higher efficiency. Various polysaccharides, such as cellulose, starch, chitosan, guar gum, and psyllium,[4–6] have been modified as hydrogels because of their use in metal-ion sorption, drug-delivery devices, and water absorption studies.[7] Chauhan et al.[8] studied the absorption of Fe^{2+} and NO_3^{-} on pine-needle-based hydrogels. In another study, Chauhan and Mahajan[9] reported that the metal-ion uptake capacities of cellulosic-based hydrogels were enhanced many times by functionalization of the anchored $-CONH_2$ with partial saponification. Shin et al.[10] used juniper bark and wood for the removal of Cd^{2+} ions from aqueous solutions at different pH values. In another study, Low et al.[11] studied the absorption of Cd^{2+} and Pb^{2+} from aqueous solution with spent grain. Kaith and Kumar[12] synthesized hybrid hydrogels based on psyllium and acrylamide (AAm) by graft copolymerization and investigated the selective absorption of water from different petroleum fraction–water emulsions as a function of time, temperature, and pH of the medium. Caykara et al.[13] synthesized ionic hydrogels based on *N,N*-dimethylacrylamide, AAm, and itaconic acid by free-radical crosslinking copolymerization in an aqueous medium with ammonium persulfate–*N,N′*-methylene bisacrylamide (MBA) as an initiator–crosslinker system and analyzed the swelling behavior of these hydrogels at various pH

Correspondence to: B. S. Kaith (bskaith@yahoo.co.in).

values. Li et al.[14] studied the synthesis of guar gum/poly(acrylic acid) semiinterpenetrating networks using MBA as a crosslinker. The kinetics of swelling and the water transport mechanism as a function of the composition of the hydrogel and the pH of the swelling medium were also studied. Zhao et al.[15] studied the synthesis of salt-, pH-, and temperature-responsive semiinterpenetrating hydrogel networks based on poly(aspartic acid) and poly(acrylic acid). Paxton and Al-Jumaily[16] proposed a modular finite element model to describe the swelling of a poly (acrylic acid) hydrogel for optical applications under the influence of an electric field. Moreover, these polymeric materials have been used extensively in agricultural and biotechnological fields. The retention of water in drought-ridden soil and pesticide delivery have been successfully achieved with these polymeric materials. These studies have shown that such natural polymers are very efficient and are of great significance in various water-treatment processes.[17,18]

In this work, we synthesized a three-dimensional crosslinked graft copolymer of acrylamide and *Gum ghatti* (Gg-*cl*-PAAm) by graft copolymerization under various pressure conditions with MBA as a crosslinking agent and a potassium persulfate (KPS)–ascorbic acid (ABC) redox pair as an initiator to investigate the impact of pressure on the superabsorbency of the candidate polymer.[19] The swelling capacity of the crosslinked product was investigated in deionized water, and the effect of the ionic strength of different cations on the swelling capacity of the hydrogel in different salt solutions was studied. Moreover, the hydrogel was used for the selective absorption of saline from different petroleum fraction–saline emulsions.

EXPERIMENTAL

Material and methods

Gum ghatti (Gg), KPS, petroleum ether, Tween 20, and ABC, procured from S. D. Fine Chemical Pvt., Ltd. (India), and MBA and AAm, purchased from Merck (India), were used as received. Petrol, diesel, and kerosene were procured from Hindustan Petroleum (India). Weighing was done on an electronic balance (Libror AEG-220, Shimadzu, India). A rotary flask shaker of Labco, Ambala (India), was used for the emulsion preparation. An autoclave (Jain Scientific Works, Ambala, India) was used to carry out the reactions under pressure.

Synthesis of Gg-*cl*-PAAm

Gg (1.0 g) was dissolved in 10 mL of deionized water for 24 h before graft copolymerization. A definite ratio of KPS and ABC followed by known amounts of AAm and MBA were added to the reaction mixture with continuous stirring. The reaction vessel was placed in the autoclave at a particular pressure. Various reaction conditions were optimized systematically. Gg-*cl*-PAAm was separated from polyacrylamide (PAAm) by precipitation of the reaction with acetone. Finally, the synthesized hybrid hydrogel was Soxhlet-extracted with acetone for about 3–4 h. To complete the gelation and three-dimensional networking, the reaction mixture was allowed to stand at room temperature for 24 h. The synthesized polymers were dried in a hot-air oven at 50°C until a constant weight was obtained. The optimization of various reaction parameters was carried out as a function of percentage grafting (P_g) and percentage swelling (P_s), which were calculated as follows:[20,21]

$$P_g = \frac{W_f - W_b}{W_b} \times 100 \quad (1)$$

where W_f and W_b are the weights of the functionalized and backbone polymers, respectively.

$$P_s = \frac{W_s - W_d}{W_d} \times 100 \quad (2)$$

where W_s and W_d are the weights of the swelled and dry polymers, respectively.

Instrumental analysis

Fourier transform infrared (FTIR) spectra of the samples were taken on PerkinElmer RXI spectrophotometer with KBr pellets (Sigma Aldrich, India). Scanning electron micrographs of the dried samples were taken on a Leo 435VF instrument (Leo Electron Microscopy, Ltd., Japan). To determine the conducting impact, the samples were gold-plated, and the scanning was synchronized with a microscopic beam to maintain the small size over a large distance relative to the specimen. The resulting images had a great depth of the field. A remarkable three-dimensional appearance with high resolution was obtained in the case of the crosslinked graft-copolymerized superabsorbent. Thermal studies of Gg and Gg-*cl*-PAAm were done on a TG/DTA 6300 SII EXSTAR 6000 (Japan). Thermogravimetric analysis (TGA) was done as a function of the percentage weight loss versus temperature at a rate of 10°C/min in air. The sample (10.0 mg) was placed in a platinum crucible to carry out the thermal analysis, with the temperature ranging from 50 to 700°C. The combustion of the sample continued for 70 min, and the results, weight loss (%) versus temperature (°C) in the case of TGA, differential thermal analysis (DTA) signal (μV) versus temperature (°C) in the case of DTA, and the rate of weight loss (mg/min) versus temperature (°C) in the case of

differential thermogravimetry (DTG), were compiled automatically by the software. The analysis was performed to examine the changes in thermal properties of Gg brought about by graft copolymerization with AAm and crosslinking with MBA. X-ray diffraction (XRD) studies of the samples were done on an X-ray diffractometer (Bruker AXS D8 Advance, Japan). XRD was performed under ambient conditions on the Bruker D_8 Advance model with Cu Kα radiation (1.5418°A), a nickel filter, and a scintillation counter as a detector at 40 kV and 40 mA on rotation between 0.5° or 1.0 mm of a divergent and antiscattering slit.

Preparation of different petroleum fraction–saline emulsions

A 1% NaCl solution was used as saline, and different emulsions of petroleum fractions and saline (1 : 1, v/v) were prepared by the addition of Tween 20 (10%) and shaking over an automatic shaking machine (Labco, India).

Swelling studies at different pH values

To investigate the swelling behavior of Gg-*cl*-PAAm at various pHs, solutions of with various pH's ranging from 3.0 to 13.0 were prepared. Alkaline and acidic solutions were prepared as per the standard methods reported in the literature.[22] The pH values were precisely checked with a Cyberscan 1100 pH meter (Eutech Instruments, India). Known amounts of the dried hydrogel were immersed in solutions of different pH, and the swelling degree was calculated with eq. (2).

Swelling studies in different salt solutions

The effects of the ionic strength and cationic charges of different cations on the swelling degree of the hydrogel were investigated in NaCl, $BaCl_2$, $FeCl_3$, and $SnCl_4$ salt solutions at preoptimized times, temperatures, and pH values in deionized water. Salt solutions of different ionic strength (0.01, 0.02, 0.03, 0.04, and 0.05 mol/L) of cations were prepared. Known amounts of the dried hydrogel were immersed in different salt solutions, and the swelling degree was calculated as per eq. (2).

Selective absorption of saline from different petroleum fraction–saline emulsions

Saline uptake studies were carried out by the immersion of 100-mg samples at a 1 : 1 petrol–saline, kerosene–saline, diesel–saline, and petroleum ether–saline emulsion ratios (100 mL). The weight of each sample was taken after a definite time interval of up to 24 h. After the optimization of time for maximum swelling degree, the sample was studied at different temperatures and a preoptimized time.

RESULTS AND DISCUSSION

Mechanism

Gg-*cl*-PAAm was synthesized through a free-radical polymerization mechanism. Hydroxyl groups present in Gg were the active sites for the formation of Gg-*cl*-PAAm. Various steps involved in the graft copolymerization process are depicted in Scheme 1.[23]

Initially, ABC reacted with persulfate to generate SO_4^{-}* [eq. (3) in Scheme 1], which, on further reaction with water molecules, gave OH*. OH* and SO_4^{-}* reacted with the monomer and backbone molecules to produce free-radical sites. Activated monomer and backbone molecules propagated the molecular chain further and gave rise to a crosslinked hybrid hydrogel in the presence of MBA.

Optimization of the various reaction parameters

The reaction time had a marked effect on P_g. Initially, P_g increased with increasing reaction time, but after it attained maxima (89%) at 6 psi, a sharp decline in P_g was observed. The increase in graft yield with time could be explained on the basis that with increasing time, interactions between SO_4^{-}* and the substrate increased and resulted in the generation of more free-radical sites on Gg and the PAAm chains. Hence, an increase in P_g was observed. However, the decrease in P_g beyond the optimum reaction time could have been due to the predominance of homopolymerization over graft copolymerization.[24] Moreover, the lesser P_g beyond the optimum reaction time may have been due to the disintegration of PAAm chains grafted onto Gg.[25,26] The optimized amount of solvent for attaining the maximum P_g (89%) was found to be 10 mL, and a further increase resulted in a lesser P_g. This could have been due to the fact that with increasing amount of solvent beyond the optimum level, the concentration of OH* decreased, and this led to the lesser generation of active sites for graft copolymerization on the backbone and monomer molecules. The pH of the reaction medium was found to have a marked effect on P_g. The maximum P_g (89%) was obtained in a neutral medium versus acidic and basic media (Table I). This could have been because of the premature termination of the polymerization with increasing pH.[27–29] Hence, a lesser P_g was observed. The molar ratio of KPS to ABC showed a marked effect on P_g. The optimized molar ratio of KPS to ABC for obtaining the maximum P_g was found to be 1 : 0.5. Initially, with increasing molar ratio, the concentrations of SO_4^{-}* and OH*

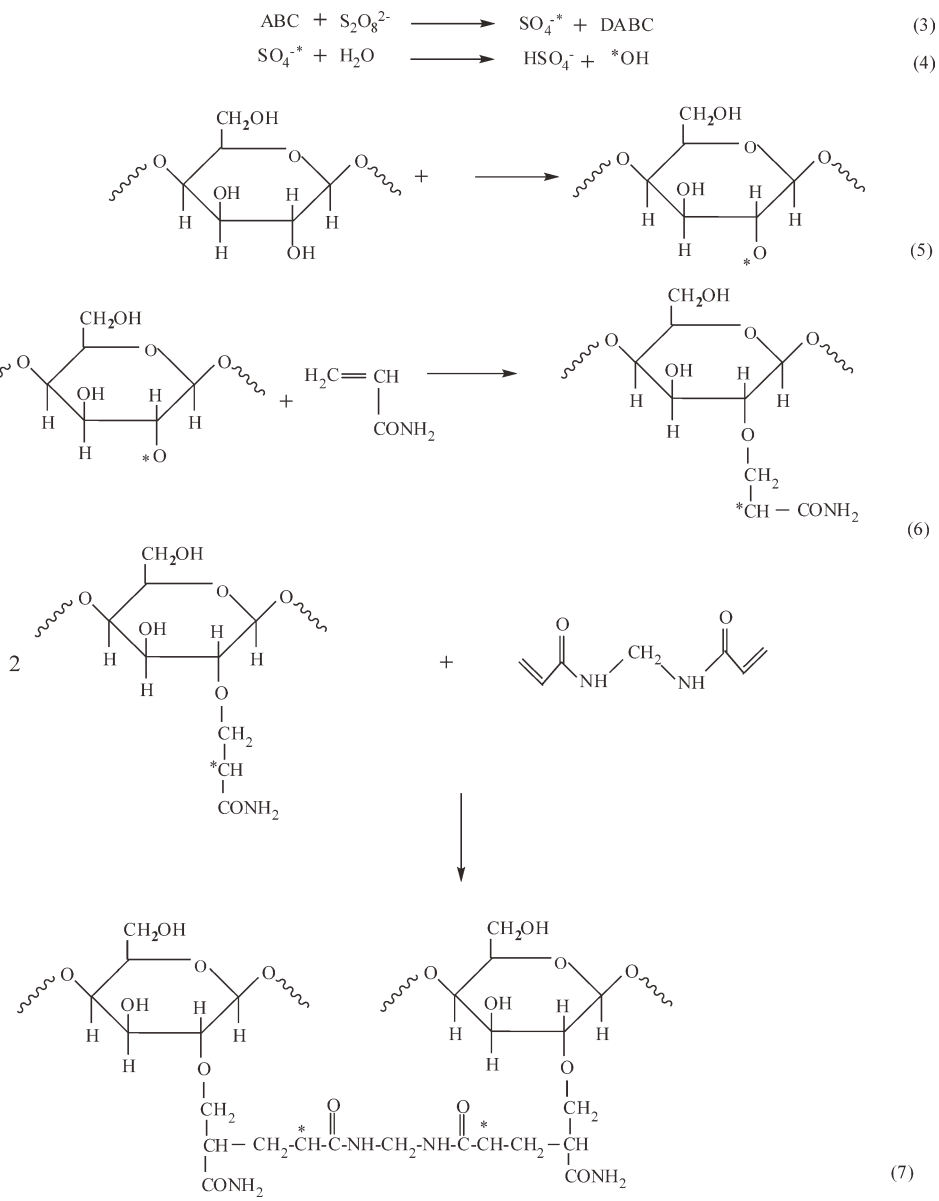

Scheme 1 Mechanism of the graft copolymerization of AAm onto Gg. DABC = dehydroascorbate.

increased, and this led to the generation of more active sites and, hence, a higher P_g. However, a further increase in the molar ratio beyond the optimum level resulted in excess SO_4^{-}* and OH*; this led to the premature termination of polymerization, and a decreased P_g was observed. Maximum P_g (97%) was observed when the reaction was carried out at a pressure of 9 psi, whereas a further increase in the pressure resulted in a decreased P_g. This might have been due to the fact that, with increased pressure, collisions between SO_4^{-}*/OH* and live propagating chains was enhanced, and this resulted in premature chain termination reactions. Hence, a decreased P_g was observed beyond 9 psi (Table I).

The optimum AAm concentration with respect to P_s was found to be 0.7042 mol/L. Initially, with increasing monomer concentration, P_s increased, but after the maximal P_s (1376%) was achieved, a further increase in the monomer concentration resulted in a decreased P_s. This might have been because of the fact that with increase in monomer concentration beyond the optimum level, the intermolecular and intramolecular self-crosslinking densities through secondary bonding forces with the porous gel structure increased; thereby, no further swelling of the hydrogel was allowed. The crosslinker concentration also had a significant effect on P_s. We observed that P_s increased with increasing crosslinker concentration, and the maximum P_s (1560%) was observed at 0.0811 mol/L. A further increase in the crosslinker concentration resulted in a decreased P_s. This could have been because of the fact that increasing the

TABLE I
Effect of Different Reaction Parameters on the P_g Values of AAm onto Gg

Sample	[AAm] (mol/L)	[MBA] (mol/L)	Time (min)	Amount of deionized water (mL)	ABC–KPS molar ratio	pH	Pressure (psi)	Mean P_g	Standard deviation	Standard error
1	0.7042	0.0649	60	10.0	1:1	7.0	6.0	29	0.87	0.50
2	0.7042	0.0649	90	10.0	1:1	7.0	6.0	43	1.56	0.90
3	0.7042	0.0649	120	10.0	1:1	7.0	6.0	58	0.90	0.52
4	0.7042	0.0649	150	10.0	1:1	7.0	6.0	71	0.66	0.38
5	0.7042	0.0649	180	10.0	1:1	7.0	6.0	89	0.90	0.52
6	0.7042	0.0649	210	10.0	1:1	7.0	6.0	69	1.14	0.66
7	0.7042	0.0649	180	5.0	1:1	7.0	6.0	45	0.86	0.49
8	0.7042	0.0649	180	7.5	1:1	7.0	6.0	65	0.83	0.48
9	0.7042	0.0649	180	12.5	1:1	7.0	6.0	63	0.50	0.28
10	0.7042	0.0649	180	15.0	1:1	7.0	6.0	47	0.76	0.44
11	0.7042	0.0649	180	17.5	1:1	7.0	6.0	32	0.63	0.36
12	0.7042	0.0649	180	10.0	1:1	1.0	6.0	35	0.80	0.46
13	0.7042	0.0649	180	10.0	1:1	3.0	6.0	58	1.10	0.63
14	0.7042	0.0649	180	10.0	1:1	5.0	6.0	73	0.95	0.54
15	0.7042	0.0649	180	10.0	1:1	9.0	6.0	65	1.11	0.64
16	0.7042	0.0649	180	10.0	1:1	11.0	6.0	42	0.56	0.32
17	0.7042	0.0649	180	10.0	0.25:1	7.0	6.0	26	0.90	0.52
18	0.7042	0.0649	180	10.0	0.5:1	7.0	6.0	47	0.36	0.21
19	0.7042	0.0649	180	10.0	0.75:1	7.0	6.0	65	1.16	0.67
20	0.7042	0.0649	180	10.0	1.25:1	7.0	6.0	38	0.48	0.28
21	0.7042	0.0649	180	10.0	1.5:1	7.0	6.0	23	0.51	0.29
22	0.7042	0.0649	180	10.0	1:1	7.0	3.0	42	0.58	0.33
23	0.7042	0.0649	180	10.0	1:1	7.0	9.0	97	1.32	0.76
24	0.7042	0.0649	180	10.0	1:1	7.0	12.0	76	0.80	0.46
25	0.7042	0.0649	180	10.0	1:1	7.0	15.0	59	0.78	0.45

Number of replications = 3 and weight of Gg = 1.0 g.

crosslinker concentration resulted in an increased density of the polymer network and, hence, lesser accessibility of the solvent toward the matrix; this, thereby, resulted in a decreased P_s (Table II).

Characterization

FTIR spectroscopy

Broad peaks were observed in the IR spectrum of Gg at 3408.4 cm^{-1} (H-bonded OH), 2936.6 cm^{-1} (C—H stretching), and 1445.35 and 1089.51 cm^{-1} (C—C and C—O stretching, respectively).

On the other hand, the IR spectrum of Gg-*cl*-PAAm showed peaks at 1635.27 cm^{-1} due to C=O stretching of the amide I band, 1469.35 cm^{-1} due to N—H in-plane bending of the amide II band, 1235.45 cm^{-1} due to C—N stretching vibrations of the amide III band, and 815.63 cm^{-1} due to OCN deformations of the amide IV band in addition to the peaks obtained with Gg [Fig. 1(a,b)]. This clearly showed that AAm and MBA formed crosslinks on Gg.[30–33]

Scanning electron microscopy (SEM)

The SEM results of Gg and Gg-*cl*-PAAm clearly show the morphological changes brought about by

TABLE II
Effect of the Monomer and Crosslinker Concentrations on the P_s Values of Gg-*cl*-PAAm

Sample	[AAm] (mol/L)	[MBA] (mol/L)	Time (min)	Amount of deionized water (mL)	KPS–ABC molar ratio	pH	Pressure (psi)	Mean P_s	Standard deviation	Standard error
1	0.563	0.0649	180	10.0	1:1	7.0	6.0	629	6.93	4.00
2	0.633	0.0649	180	10.0	1:1	7.0	6.0	967	4.58	2.65
3	0.7042	0.0649	180	10.0	1:1	7.0	6.0	1376	6.25	3.61
4	0.7746	0.0649	180	10.0	1:1	7.0	6.0	916	5.58	3.21
5	0.845	0.0649	180	10.0	1:1	7.0	6.0	734	3.61	2.08
6	0.7042	0.0487	180	10.0	1:1	7.0	6.0	756	5.00	2.89
7	0.7042	0.0811	180	10.0	1:1	7.0	6.0	1560	3.00	1.73
8	0.7042	0.0974	180	10.0	1:1	7.0	6.0	1061	3.46	2.00
9	0.7042	0.1136	180	10.0	1:1	7.0	6.0	654	3.61	2.08

Number of replications = 3 and weight of Gg = 1.0 g.

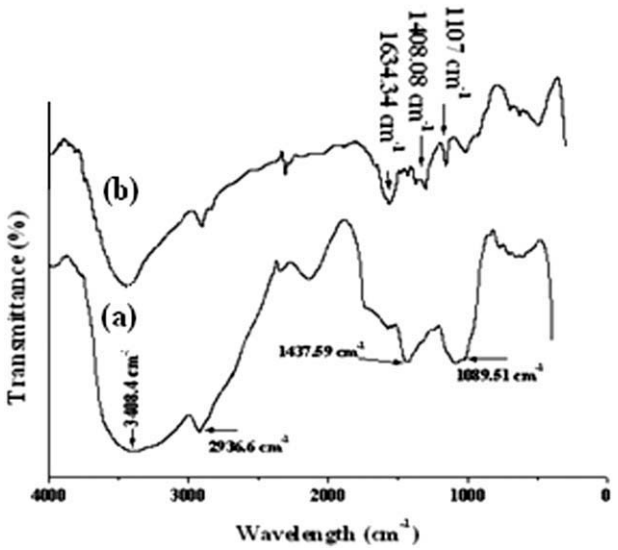

Figure 1 FTIR spectra of (a) Gg and (b) Gg-*cl*-PAAm.

crosslinking with MBA. The morphological changes in the features of Gg after grafting and networking revealed a clear distinction between the crosslinked product and the backbone [Fig. 2(a,b)].[24,32,34]

TGA, DTA, and DTG studies

In the case of TGA of Gg, a two-stage decomposition was observed. The first-stage decomposition was due to an initial breakdown of the crosslinked network,[35] whereas the second-stage decomposition was due to depolymerization reactions. The first-stage decomposition was observed in the temperature range from 206.9 to 331.4°C with 46.6% weight loss, and the second-stage decomposition was observed in the temperature range from 331.4 to 521.6°C with 31.2% weight loss. Gg exhibited an initial decomposition temperature (IDT) of 206.9°C and a final decomposition temperature (FDT) of 521.6°C. Two exothermic peaks at 483.2°C (203 μV) and 492.7°C (154 μV) were obtained in the case of DTA of Gg. DTG of Gg showed decompositions at 299.1 and 479.0°C with 1.463 and 2.230 mg/min weight loss, respectively [Fig. 3(a)].

It was observed that the IDT of Gg-*cl*-PAAm (157.2°C) was lower than that of Gg (206.9°C). However, FDT of Gg-*cl*-PAAm was higher than that of Gg. A two-stage decomposition ranging from 157.2 to 357.2°C and 357.2 to 601.3°C was observed [Fig. 3(b)]. In the case of DTA, one endothermic peak at 175.9°C (−5.4 μV) and one exothermic peak at 588.4°C (154.4 μV) was observed; these showed that the exothermic combustion of Gg-*cl*-PAAm persisted at a higher temperature compared to that of Gg. The DTG curve showed variations in the weight loss rate of 0.37 mg/min at 160.7°C, 0.45 mg/min at 230.7°C, and 0.33 mg/min at 381.4°C corresponding to the first-stage decomposition of TGA and 1.049 mg/min at 580.5°C corresponding to the second-stage decomposition of TGA (Table III).[30–32,36] Because the FDT of the crosslinked network (601.3°C) was found to be higher than that of the backbone (521.6°C), a higher thermal stability was observed from the grafting and crosslinking of Gg with AAm–MBA.

XRD studies

The coherence length (L) of the samples was calculated with the Scherrer equation:[37,38]

$$L = 0.9\lambda/\beta_{1/2}\cos\theta$$

where λ is the wavelength, θ is the diffraction angle, and $\beta_{1/2}$ is the full width at half-maximum.

Gg was found to be the least crystalline among its crosslinked products with the lowest value of L. It is evident from Table IV that, in the case of Gg-*cl*-PAAm, in the crosslinked networks with MBA concentrations of 0.0478, 0.0649, 0.0811, 0.0974, and

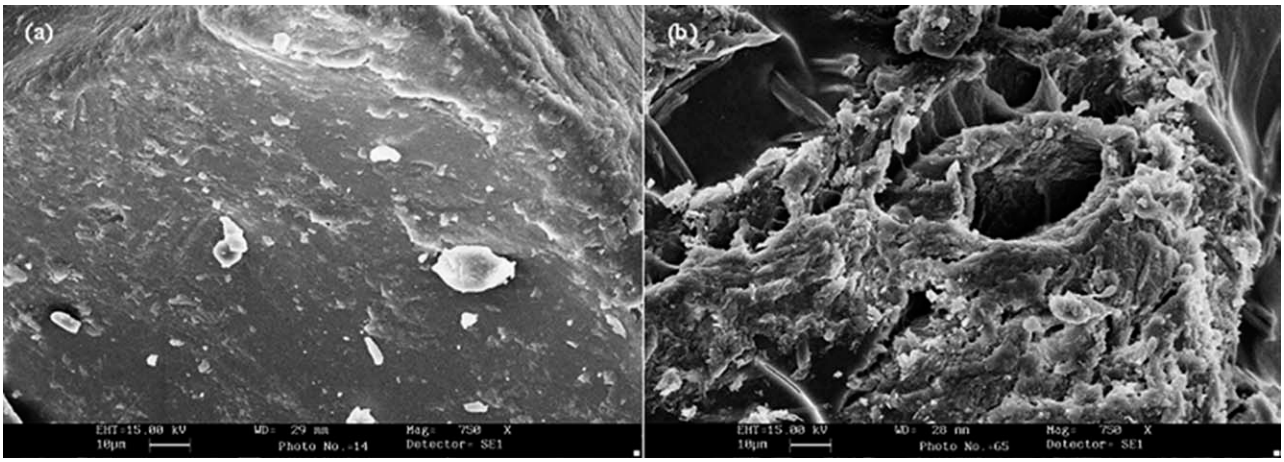

Figure 2 SEM micrographs of (a) Gg and (b) Gg-*cl*-PAAm.

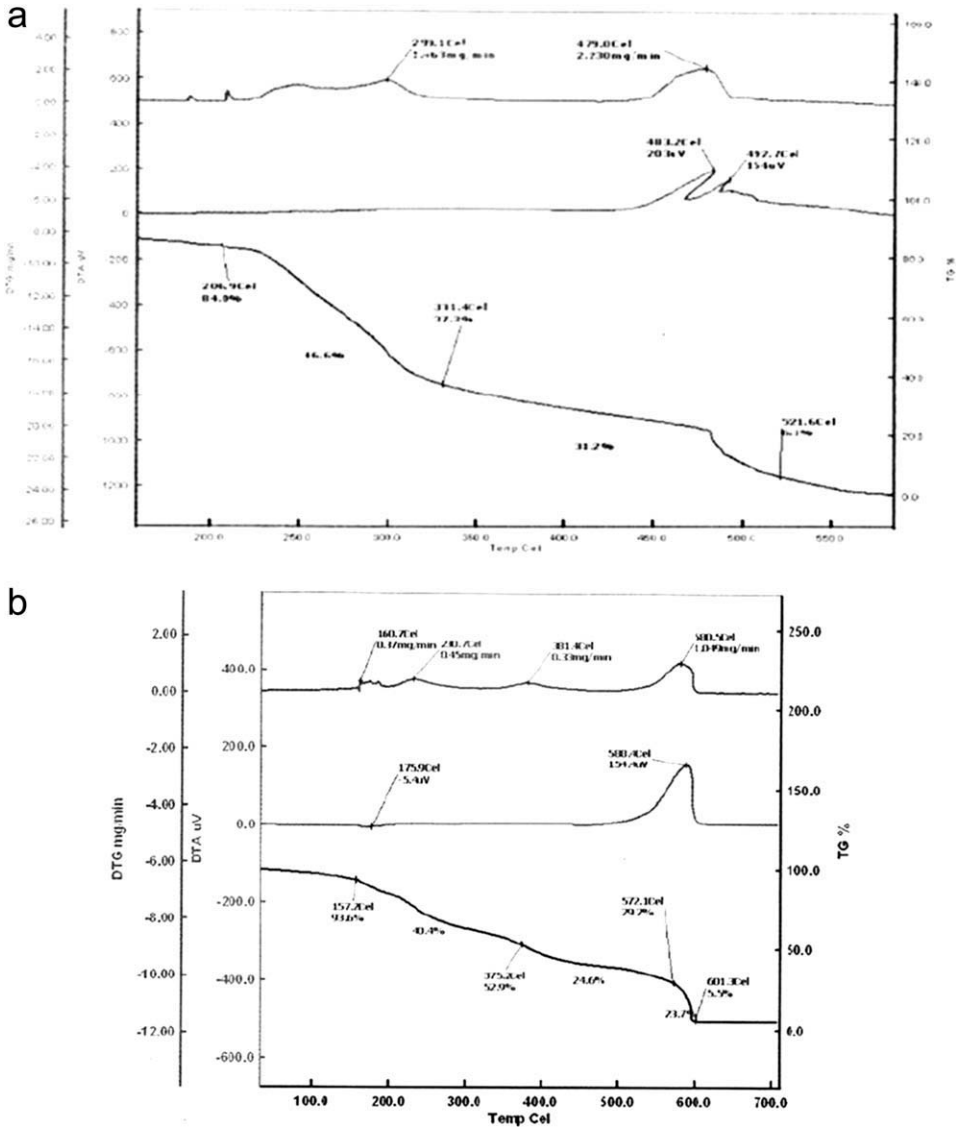

Figure 3 TGA of (a) Gg and (b) Gg-*cl*-PAAm (TG = thermogravimetry).

0.1136 mol/L, the maximum intensity peaks corresponded to 2θ values of 25.452° (L = 1.731Å), 24.972° (L = 1.776Å), 24.335° (L = 1.849 Å), 20.790° (L = 1.941 Å), and 19.337° (L = 2.024 Å), respectively, whereas the Gg maximum intensity peak corresponded to 2θ = 20.908° (L = 1.057 Å). Thus, L was found to increase with increasing crosslinker concentration, and this resulted in increased anisotropy. Hence, the polymer became more crystalline in nature. This might have been to the fact that with increasing crosslinker concentration, the crosslinker density between polymeric chains increased; this led to a more aligned crystalline structure.[38]

Absorption studies in deionized water

Absorption studies of Gg-*cl*-PAAm in deionized water were carried out as a function of time, temperature, and pH of the medium.

Effect of the time on P_s

Figure 4(a) reveals the effect of time onto P_s for Gg-*cl*-PAAm. It was observed that the swelling degree kept on increasing with time, and the maximum swelling ratio (1742%) was found at a time interval of 16 h. A further increase in the swelling time showed no more increase in the equilibrium swelling. This was due to the fact that with increasing time interval, the porous network of the polymer became fully saturated, with no more accommodation for the solvent molecules.[39]

Effect of the temperature on P_s

The effect of the temperature on the swelling degree of the candidate polymer was investigated at different temperatures (30, 40, 50, 60, and 70°C) and at a preoptimized time [16 h; Fig. 4(b)]. It was observed

TABLE III
Thermal Behavior of Gg and Gg-*cl*-PAAm

Sample code	TGA				DTA		DTG	
	IDT	First-stage decomposition temperature (% weight loss)	Second-stage decomposition temperature (% weight loss)	FDT (residue left)	Exothermic peaks at different decomposition temperatures (μV)		Decomposition temperature (rate of weight loss; mg/min)	
					First	Second	First	Second
Gg	206.6°C	206.9–331.4°C (46.6%)	331.4–521.6°C (32.5%)	521.6°C	483.2°C (203)	492.7°C (154)	299.1°C (1.463)	470.0°C (2.230)
Gg-*cl*-PAAm	152.7°C	152.7–375.2°C (40.4%)	375.2–601.3°C (48.3%)	601.3°C (5.5%)	175.9°C	588.4°C (154.4)	160.7°C (0.37)	580.5°C (1.049)

that, initially, the swelling degree increased with increasing temperature and attained a maximum at 60°C. A further increase in the temperature resulted in no further increase in the swelling degree. This might have been because of the fact that, with increasing temperature, the elasticity of the polymeric matrix increased; this resulted in increased swelling, but after the optimum temperature was reached, the matrix started collapsing, and this led to desorption with further increases in temperature.[39] Furthermore, water molecules formed hydrogen bonds with the hydrophilic groups of the candidate polymer; this led to the stable shell of hydration around these hydrophilic groups and resulted in a greater absorption of water and a larger swelling degree, However, at higher temperatures, the associated interactions among the hydrophilic groups released the entrapped water molecules from the hydrogel network.[40,41]

Effect of pH on P_s

Swelling studies of Gg-*cl*-PAAm were carried out at different pHs (3.0–13.0) and at a preoptimized time (16 h) and temperature (60°C) [Fig. 4(c)]. The maximum swelling degree (1350%) was observed at pH 7.0, whereas lesser swelling degrees were observed in acidic and alkaline media. This type of behavior could be explained on the basis of osmotic swelling pressure (π_{ion}).[42] For a weakly charged hydrogel network, π_{ion} is given as follows:

$$\pi_{ion} = RT\Sigma(C_i^g - C_i^s)$$

where C_i^g and C_i^s are the molar concentrations of mobile ions in the swollen gel and external solution, respectively; R is the gas constant; and T is the absolute temperature.

As glucoronic acid is one of the components of Gg,[43] it is composed of carboxylate groups (COO^-) along the polymer chain. In neutral media, C_i^s is almost negligible; therefore, π_{ion} becomes almost very large; this leads to a larger swelling degree. Moreover, the electrostatic repulsion between carboxylate ions increases the swelling degree in neutral media, whereas, in acidic media, π_{ion} becomes very small because the carboxylate ions within the swollen gel get protonated. This results in a low value of C_i^s.[22] Also, in acidic media, carboxylate ion repulsion is screened by H^+ ions, which do not allow the network to expand and result in a decreased swelling degree. On the other hand, in an alkaline solution, the dissociation of —COOH group is almost complete, but a very high concentration of Na^+ and ^-OH ions leads to reductions in π_{ion} and P_s. Also, a higher concentration of Na^+ ions acts as a screening bar and, thereby, reduces the repulsion

TABLE IV
Effect of the Concentration of MBA on *L*

Sample code	MBA (mol/L)	*d*-Spacing	Angle of diffraction at 2θ scale (°)	$\beta_{1/2}$ at 2θ scale (°)	*L* (nm)
Gg	—	4.24532	20.908	13.17	1.057
Gg-*cl*-PAAm (I)	0.0478	3.4967	25.452	7.9723	1.731
Gg-*cl*-PAAm (II)	0.0649	3.5692	24.927	7.9195	1.776
Gg-*cl*-PAAm (III)	0.0811	3.6547	24.335	7.4085	1.849
Gg-*cl*-PAAm (IV)	0.0974	4.2692	20.790	7.0920	1.941
Gg-*cl*-PAAm (V)	0.1136	4.5866	19.337	6.7810	2.024

between different carboxylate groups; hence, a lesser swelling degree will be observed.

Swelling–deswelling–reswelling behavior

Figure 4(d) reveals the effect of changing pH on the swelling–deswelling–reswelling behavior of the hydrogels. The ability of the candidate polymer to exhibit reversibility in swelling behavior was examined in the solutions of pH 3.0 and 8.0. It was observed that, when the hydrogel was immersed in a solution of pH 8.0m swelling occurred because of anion–anion repulsion; however, when the swollen hydrogel was placed in a solution of pH 3.0, it deswelled because of protonation of the carboxylate groups. Now, again, when the deswelled hydrogel was placed in a solution of pH 8.0, it swelled again and, thereby, exhibited pulsatile behavior.[44,45]

Effect of the ionic strengths of different cations on P_s

Figure 4(e) shows the swelling data obtained from the chloride salt solutions of various cations with different ionic strengths. From the figure, it is clear that swelling degree decreased with increasing charge of the metal cation ($Na^+ > Ba^{2+} > Fe^{3+} > Sn^{4+}$). Although, initially, the candidate polymer showed swelling behavior in each salt solution, after a certain time interval, a definite difference in the

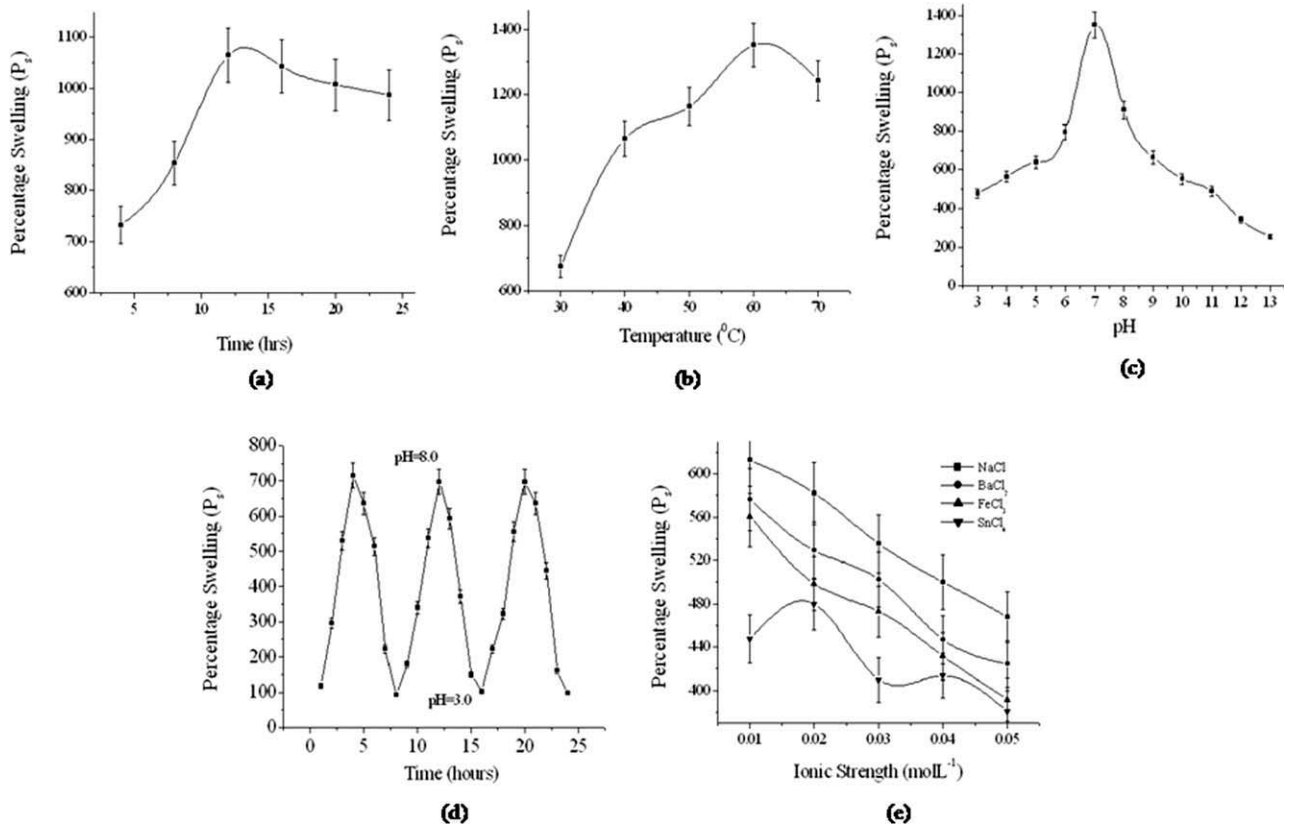

Figure 4 (a) Effect of the time on P_s in deionized water, (b) effect of the temperature on P_s in deionized water, (c) effect of pH on P_s in deionized water, (d) pulsatile behavior of Gg-*cl*-PAAm, and (e) effect of the ionic strengths of different cations on P_s in different salt solutions.

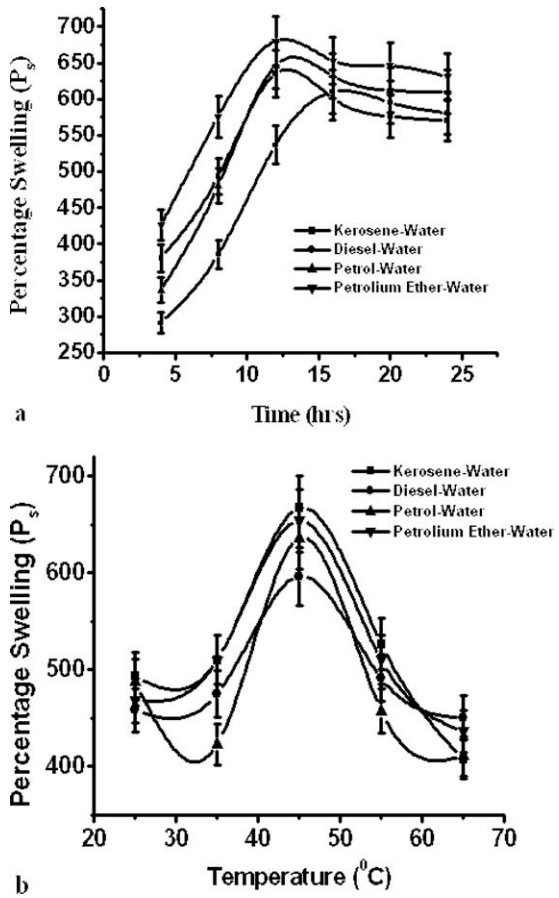

Figure 5 Effects of the (a) time and (b) temperature on P_s in different petroleum fraction–saline emulsions.

swelling behavior of the candidate polymer in different salts was observed. This could have been due to the fact that, as the ionic charge increased, there was a proportionate increase in the cation–cation repulsion, which did not allow more entry of solution containing cations inside the crosslinked network; this, thereby, resulted in the desorption of ions. This ultimately led to a decreasing trend in the swelling behavior of the candidate polymer.[20] It was further observed that the swelling degree of the candidate polymer decreased with increasing ionic strength of the cation in the respective salt solutions. A decrease in the swelling degree with increasing ionic strength of the cations was due to a reverse osmosis process.[46]

Selective saline absorption studies from different petroleum fraction–saline emulsions

Effect of the time

Saline absorption studies were carried out at different time intervals (4, 8, 12, 16, 20, and 24 h) as a function of the swelling degree. Initially, the swelling degree increased with increasing time interval up to 12 h, and the maximum swelling degrees were found to be 635, 636, 646, and 680% for kerosene–saline, diesel–saline, petrol–saline, and petroleum ether–saline emulsions, respectively. After 16 h, the porous network of the gel became saturated, and absorption was found to almost cease [Fig. 5(a)].[39]

Effect of temperature

Saline absorption studies of the candidate polymer were carried out at a preoptimized time (12 h) while the temperature of the absorption media was varied from 25 to 65°C. The maximum absorption was observed at 45°C. The maximum P_s values in kerosene–saline, diesel–saline, petrol–saline, and petroleum ether–saline emulsions were found to be 667, 596, 636, and 654% [Fig. 5(b)], respectively. However, a further increase in temperature resulted in decreased absorption; this might have been because of the fact that at elevated temperature, the polymer started collapsing because of disintegration and desorption processes.[39]

CONCLUSIONS

Modification of Gg via graft copolymerization and network formation with AAm improved the property profile and usability of the polymer for various technical fields. The crosslinked product was found to be thermally more stable than the initial backbone polymer. This polymer network showed selective water absorption in all of the different petroleum fraction–saline emulsions, as it failed to swell in petrol, diesel, kerosene, and petroleum ether. Hence, it makes the candidate polymer suitable for the oil industry. Thus, the functionalized polymer is important from a technological viewpoint.

The authors are very thankful to the faculty of Himachal Pradesh University, Summer-Hill, Shimla, India, for their encouragement throughout the course of this work and the Institute Instrumentation Center, Indian Institute of Technology (IIT) Roorkee, for their cooperative behavior during the characterization of the samples.

References

1. Sahiner, N. Eur Polym J 2007, 43, 1709.
2. Hoffman, A. S. Adv Drug Deliv Rev 2002, 43, 3.
3. Buchholz, F. L.; Graham, A. T. Modern Superabsorbent Polymer Technology; Wiley: New York, 1998.
4. Lu, S.; Yao, K.; Lin, S.; Cao, D.; Chen, Y. Starch-Starke 2003, 55, 518.
5. Peng, X.; Zhang, L.; Kennedy, J. F. Carbohydr Polym 2006, 65, 288.
6. Trivedi, J. H.; Kalia, K.; Patel, N. K.; Trivedi, H. C. Carbohydr Polym 2005, 60, 117.
7. De, S. K.; Aluru, N. R.; Johnson, B.; Crone, W. C.; Beebe, D. J.; Moore, J. J Microelectromech S 2002, 11, 544.
8. Chauhan, G. S.; Chauhan, S.; Kumar, S.; Kumari, A. Bioresour Technol 2008, 99, 6464.

9. Chauhan, G. S.; Mahajan, S. J Appl Polym Sci 2002, 86, 667.
10. Shin, E. W.; Karthikeyan, K. G.; Tshabala, M. A. Bioresour Technol 2007, 98, 5888.
11. Low, K. S.; Lee, C. K.; Liew, S. C. Proc Biochem 2000, 36, 59.
12. Kaith, B. S.; Kumar, K. Bull Mater Sci 2007, 30, 387.
13. Caykara, T.; Kiper, S.; Demirel, G. Eur Polym J 2006, 42, 348.
14. Li, X.; Wu, W.; Wang, J.; Duan, Y. Carbohydr Polym 2006, 66, 473.
15. Zhao, Y.; Kang, J.; Tan, T. Polymer 2006, 47, 7702.
16. Paxton, R. A.; Al-Jumaily, A. M. Polymer 2006, 47, 5997.
17. Adeloju, S. B.; Wallace, G. G. Analyst 1996, 121, 699.
18. Azzam, R. A. I. Commun Soil Sci Plan 1980, 11, 767.
19. Kalia, A.; Kaith, B. S. J Chil Chem Soc 2009, 54, 108.
20. Kalia, S.; Kaith, B. S. Int J Polym Anal Ch 2008, 13, 341.
21. Pourjavadi, A.; Mahdavinia, G. R. Turk J Chem 2006, 30, 595.
22. Mahdavinia, G. R.; Pourjavadi, A.; Hosseizadeh, H.; Zohuriaan, M. J. Eur Polym J 2004, 40, 1399.
23. Pourjavadi, A.; Barzegar, S.; Mahdavinia, G. R. Carbohydr Polym 2006, 66, 386.
24. Mishra, A.; Clark, J. H.; Pal, S. Carbohydr Polym 2008, 72, 608.
25. Tian, D.; Xie, H. Q. Polym Bull 2008, 61, 277.
26. Akgun, S.; Ekici, G.; Mutlu, N.; Besirli, N.; Hazer, B. J Polym Res 2007, 14, 215.
27. Kaith, B. S.; Jindal, R.; Maiti, M. J Appl Polym Sci 2009, 113, 1781.
28. Kaith, B. S.; Jindal, R.; Jana, A.; Maiti, M. Carbohydr Polym 2009, 78, 987.
29. Kaith, B. S.; Jindal, R.; Jana, A.; Maiti, M. Iran Polym J 2009, 18, 789.
30. Nayak, B. R.; Biswal, D. R.; Karmakar. N. C.; Singh, R. Bull Mater Sci 2002, 25, 537.
31. Bardajee, G. R.; Pourjavadi, A.; Soleyman, R.; Sheikh, N. Nucl Instrum Methods B 2008, 266, 3932.
32. Singh, V.; Tiwari, A.; Tripathi, D. N.; Sanghi, R. Carbohydr Polym 2004, 58, 1.
33. Pourjavadi, A.; Kurdtabar, M. Eur Polym J 2007, 43, 877.
34. Sen, G.; Kumar, R.; Ghosg, S.; Pal S. Carbohydr Polym 2009, 77, 822.
35. Ranjata, S. Ph.D. Thesis, National Institute of Technology, Hamirpur, India, 2010.
36. Singh, V.; Tripathi, D. N.; Tiwari, A.; Sanghi, R. Carbohydr Polym 2006, 65, 35.
37. Patteron, A. L. Phys Rev 1939, 56, 978.
38. Malik, H.; Gupta, N.; Sarkar, A. Mater Sci Eng C 2002, 20, 215.
39. Kaith, B. S.; Kumar, K. Iran Polym J 2007, 16, 529.
40. Xu, F. J.; Kang, E. T.; Neoh, K. G. Biomaterials 2006, 27, 2787.
41. Feil, H.; Bae, Y. H.; Feijen, J.; Kim, S. W. Macromolecules 1993, 26, 2496.
42. Bajpai, S. K. Iran Polym J 1999, 8, 231.
43. Aspinall, G. O. In the Biochemistry of Plants, 3rd ed.; Preiss, J., Ed.; Academic: New York, 1980; p 473.
44. Guo, J.; Li, L.; Ti, Y.; Zhu, J. eXPRESS Polym Lett 2007, 1, 166.
45. Kim, S. J.; Yoon, S. G.; Lee, S. M.; Lee, L. H.; Kim, S. I. Sens Actuators B 2003, 96, 1.
46. Kaith, B. S.; Ranjata, S.; Kumar, K. e-Polymers 2008, no. 158.